Iranian Journal of Basic Medical Sciences
ijbms.mums.ac.ir

Huanglian Jiedu decoction ameliorates Alzheimer's disease by regulating calcium homeostasis via mitochondria-associated endoplasmic reticulum membranes

Yong Yuan [1], Zhonghua Li [1]*, Ruifang Wang [1], Huandong Zhao [1], Junying Song [1]*

[1] Academy of Chinese Medical Sciences; Collaborative Innovation Center of Research and Development on the Whole Industry Chain of Yu-Yao, Henan University of Chinese Medicine, Zhengzhou 450046, China

ARTICLE INFO

Article type:
Original

Article history:
Received: Oct 11, 2025
Accepted: Mar 8, 2026

Keywords:
Alzheimer's disease
Amyloid beta-peptides- (1-42)
Calcium
Huanglian Jiedu decoction
Mitochondria-associated-membranes (MAMs)

ABSTRACT

Objective(s): Huanglian Jiedu decoction (HLJDD), a classic traditional Chinese medicine formula, is investigated for its protective effects against Alzheimer's disease (AD). This study explored its mechanism in an AD cell model, focusing on calcium ion (Ca^{2+}) homeostasis regulation via mitochondria-associated endoplasmic reticulum membranes (MAMs).

Materials and Methods: Mouse hippocampal HT22 cells were induced with 10 μmol·L^{-1} $A\beta_{1-42}$ to establish the AD model, then divided into blank, model, and 15% HLJDD-containing serum intervention groups. Fluorescent dyes, qRT-PCR, western blotting, laser scanning confocal microscopy, and Annexin V-FITC/PI staining were used to detect intracellular reactive oxygen species (ROS), mitochondrial membrane potential, VDAC1/GRP75/IP3R (mRNA/protein levels), MAMs formation, intracellular Ca^{2+}, and cell apoptosis, respectively.

Results: $A\beta_{1-42}$ reduced HT22 viability in a concentration-dependent manner, while HLJDD significantly improved viability. Compared to the model group, HLJDD evidently decreased ROS levels (P<0.001), elevated mitochondrial membrane potential (P<0.001), up-regulated GRP75 (mRNA/protein, P<0.05), down-regulated VDAC1/IP3R (mRNA/protein, P<0.05 or P<0.001), reduced MAMs (via lower ER-mitochondria co-localization, P<0.05), alleviated Ca^{2+} overload (P<0.001), and lowered apoptosis.

Conclusion: HLJDD exerts protective anti-AD effects likely by reducing MAMs formation to alleviate intracellular Ca^{2+} overload, thereby lessening cell damage and apoptosis.

▶Please cite this article as:
Yuan Y, Li Zh, Wang R, Zhao H, Song J. Huanglian Jiedu decoction ameliorates Alzheimer's disease by regulating calcium homeostasis via mitochondria-associated endoplasmic reticulum membranes. Iran J Basic Med Sci 2026; 29:

Introduction

Alzheimer's disease (AD) stands as a pressing global healthcare challenge, characterized by progressive cognitive decline and neuronal loss that impose profound burdens on patients, caregivers, and healthcare systems. According to World Alzheimer's Report in 2023, AD is now ranked the seventh leading cause of death worldwide, and demographic projections estimate that the global prevalence of AD will surge to 139 million cases by 2050 (1). Despite decades of intensive research, the translational landscape for AD therapeutics remains bleak. Traditional strategies targeting β-amyloid (Aβ) aggregation or tau hyperphosphorylationhave consistently failed in late-stage clinical trials. For example, recent phase III studies of anti-Aβ monoclonal antibodies demonstrated only modest improvements in cognitive function, accompanied by adverse effects such as amyloid-related imaging abnormalities, highlighting the need to move beyond the "amyloid cascade" hypothesis and explore alternative pathological mechanisms (2-4).

Against this backdrop of unmet therapeutic needs, exploring emerging pathological pathways that integrate multiple AD-related cascades has become a research priority. Among these pathways, mitochondria-associated membranes (MAMs)-specialized lipid-rich contact sites between the endoplasmic reticulum (ER) and mitochondria, have emerged as a central integrator of AD-related pathologies. Unlike isolated organellar dysfunction, MAMs regulate bidirectional crosstalk between the ER and mitochondria, governing critical cellular processes, including energy metabolism, ER stress resolution, and intracellular calcium (Ca^{2+}) signaling (5, 6). MAMs are particularly relevant to AD because key disease-related molecules are spatially enriched at these sites. These molecules include γ-secretase, an enzyme complex that cleaves amyloid precursor protein (APP) into neurotoxic Aβ peptides. Its catalytic subunit, presenilin, is also highly concentrated at MAMs. This localization

Corresponding authors: Zhonghua Li. Academy of Chinese Medical Sciences; Collaborative Innovation Center of Research and Development on the Whole Industry Chain of Yu-Yao, Henan University of Chinese Medicine, Zhengzhou 450046, China. Email: lizh@hactcm.edu.cn; Junying Song. Academy of Chinese Medical Sciences; Collaborative Innovation Center of Research and Development on the Whole Industry Chain of Yu-Yao, Henan University of Chinese Medicine, Zhengzhou 450046, China. Email: junying1206@126.com

suggests MAMs may serve as a molecular hotspot for Aβ production, but more importantly, preclinical and clinical studies have documented aberrant MAMs activity in AD. Postmortem analyses of AD brains, as well as studies in APP/PS1 transgenic mice and Aβ-induced cellular models, show increased ER-mitochondria co-localization and dysregulated MAMs function. This hyperactive MAMs phenotype is not a secondary consequence of Aβ or tau pathology; instead, it drives downstream pathological cascades, including mitochondrial Ca^{2+} overload, reactive oxygen species (ROS) overproduction, and neuronal apoptosis (7, 8).

Disruption of Ca^{2+} homeostasis represents a common pathway leading to neuronal death in AD, with its dysregulation amplifying Aβ-induced neurotoxicity, ROS accumulation, and neuroinflammation (9). MAMs serve as the primary platform for controlled Ca^{2+} transfer from the ER to mitochondria, a process mediated by the IP3R-Grp75-VDAC protein complex. In this complex, inositol 1,4,5-trisphosphate receptors (IP3Rs) on the ER membrane bind to glucose-regulated protein 75 (Grp75), an adapter protein that links IP3Rs to voltage-dependent anion channels (VDACs) on the outer mitochondrial membrane. This functional channel ensures precise Ca^{2+} flux, which is essential for maintaining mitochondrial bioenergetics (10). In AD, hyperactive MAMs increase IP3R-VDAC interaction, leading to excessive Ca^{2+} influx into mitochondria. This mitochondrial Ca^{2+} overload impairs oxidative phosphorylation, triggers ROS generation, and activates apoptotic pathways, which all contributors to neuronal loss. Supporting the therapeutic potential of targeting this axis, preclinical studies have shown that down-regulating IP3R expression in astrocytes reduces intracellular Ca^{2+} levels, attenuates $A\beta_{1-42}$-induced ER stress, and reverses learning-memory deficits and synaptic dysfunction in APP/PS1 mice (11). Similarly, Naohuan Pan, a traditional Chinese medicine (TCM) formulation, improves cognitive function in AD mice by normalizing hippocampal Ca^{2+} concentrations, likely through modulation of MAMs-related Ca^{2+} transporters (12). These findings collectively validate MAMs-mediated Ca^{2+} homeostasis as a viable therapeutic target for AD.

Against this backdrop, TCM formulations offer a unique avenue for AD therapy, with HuanglianJiedu Decoction (HLJDD) standing out as a promising candidate. HLJDD is a classic TCM formula with a 1,700-year clinical legacy, first described in *ZhouhouBeiji Fang* by Ge Hong (Eastern Jin Dynasty) and later formalized in *Waitai Miyao* by Wang Tao (Tang Dynasty) (13). Its application in AD is rooted in the TCM theory of "toxin damaging the brain collaterals," where toxin refers to pathological factors that disrupt physiological balance and induce irreversible tissue damage, a concept that aligns with modern understanding of AD-related neurotoxins (e.g., Aβ, ROS, and proinflammatory cytokines)(14, 15). Preclinical evidence confirms HLJDD's efficacy in AD models. For example, Zhang *et al.* showed HLJDD ameliorates learning and memory deficits in APP/PS1 mice by down-regulating hippocampal HIF-1α and VEGF to exert neuroprotection (16); it alleviates neuronal damage in Tau/APP/PS1 mice by inhibiting NLRP3 inflammasome activation and microglial overactivation to reduce Aβ40, Aβ42 and p-Tau levels (17); it also enhances cognitive function and protects neurons in 8-month-old APP/PS1 mice by suppressing urea metabolism-related ODC1 expression in hippocampal astrocytes to inhibit astrocyte hyperactivation and toxic GABA production (18). Despite these advances, the precise molecular mechanisms of HLJDD in AD remain unclear, particularly whether it targets mitochondria-associated endoplasmic reticulum membranes (MAMs)-mediated Ca^{2+} homeostasis.

To fill this gap, the present study established an *in vitro* AD model by treating HT22 hippocampal neurons with $A\beta_{1-42}$, the most neurotoxic Aβ isoform. We then investigated the effects of HLJDD on MAMs structure, MAMs-related Ca^{2+} transporters, intracellular and mitochondrial Ca^{2+} levels, and downstream pathological events. Our central hypothesis is that HLJDD mitigates $A\beta_{1-42}$-induced neurotoxicity by normalizing MAMs function and restoring Ca^{2+} homeostasis. By elucidating this mechanism, we aim to provide experimental evidence for HLJDD's clinical application in AD and advance the understanding of TCM formulations as targeted therapies for neurodegenerative diseases.

Materials and Methods

Experimental materials

The medicinal herbs of HLJDD, including Huanglian (*Coptidis Rhizoma*), Huangqin (*Scutellariae Radix*), Huangbai (Phellodendri Cortex), and Zhizi (*Gardeniae Fructus*), were all purchased from Zhang Zhongjing Pharmacy, Zhengzhou City, Henan Province. They were identified as authentic samples by Professor Tao Guo from the School of Pharmacy, Henan University of Chinese Medicine. Each component was prepared into an aqueous decoction according to the drug ratio (9:6:6:9) specified in the *Chinese Pharmacopoeia* (2020 Edition), and concentrated to a mass concentration of 1 $g \cdot ml^{-1}$ for later use.

$A\beta_{1-42}$ (Shanghai Qiangyao Biotechnology Co., Ltd., Catalog No.: 04010011526); Mouse hippocampal neuronal HT22 cell line (Wuhan Procell Life Science & Technology Co., Ltd., Catalog No.: CL-0595).

Main reagents

DMEM high-glucose medium, MTT, RIPA lysis buffer, protease inhibitor (PMSF), BCA kit, PVDF membrane (Beijing Solarbio Science & Technology Co., Ltd., Catalog Nos.: 12100, M8180, R0010, P0100, PC0020, YA1701 respectively); DCFH-DA reactive oxygen species (ROS) fluorescent probe (Shanghai Yisheng Biotechnology Co., Ltd., Catalog No.: 50101ES01); Mitochondrial red fluorescent probe, endoplasmic reticulum (ER) green fluorescent probe, enhanced mitochondrial membrane potential detection kit (Shanghai Biyuntian Biotechnology Co., Ltd., Catalog Nos.: C1049B, C1042S, C2003S respectively); Rhod-2, AM calcium ion fluorescent probe (Shanghai Maokang Biotechnology Co., Ltd., Catalog No.: MX4507); Annexin V-FITC/PI cell apoptosis detection kit (Wuhan Elabscience Biotechnology Co., Ltd., Catalog No.: E-CK-A211); VDAC1 and GRP75 antibodies (Proteintech Group, Inc., Catalog Nos.: 14887-1-AP, 55259-1-AP respectively); IP3R antibody (GeneTex, Inc., USA, Catalog No.: GTX637015); Rabbit anti-β-actin polyclonal antibody (Beijing Abways Biotechnology Co., Ltd., Catalog No.: P60709); Glass-bottom cell culture dish (Wuxi NEST Biotechnology Co., Ltd., Catalog No.: 801002).

Main instruments and equipment

Multifunctional full-wavelength microplate reader (Thermo Fisher Scientific, Inc., USA, Model: MultiskanGO); Quantitative real-time PCR (qPCR) instrument (Roche Diagnostics GmbH, USA, Model: LightCycler 96); Electrophoresis apparatus (Bio-Rad Laboratories, Inc., USA, Model: JY200C); High-speed refrigerated centrifuge (Beckman Coulter, Inc., USA, Model: Microfuge®20R); Laser scanning confocal microscope (Leica Microsystems GmbH, Germany, Model: STELLARIS 5); Flow cytometer (Becton, Dickinson and Company, USA, Model: FACSCanto II).

Preparation of HLJDD-containing serum

Twenty SPF-grade mice were randomly divided into a control group and HLJDD administration group, with 10 mice per group. All mice were acclimatized for 3 days prior to the experiment. The administration group received HLJDD via intragastric gavage at a dose of 5 g/kg per day. The actual gavage volume was adjusted according to the body weight of individual mice and the concentration of the HLJDD solution. For the control group, an equal volume of normal saline was administered by gavage Gavage was performed twice daily for 7 consecutive days. Two hours after the final gavage, blood samples were collected via the eyeball enucleation method. The collected blood was centrifuged to separate the serum, and the serum samples from mice within the same group were pooled. The pooled serum was incubated at 56 ˚C for 30 min, subjected to filtration sterilization, and then stored at -80 ˚C until subsequent experiments.

MTT assay for cell viability

Logarithmic-phase HT22 cells were seeded into two 96-well plates at 1×10^4 cells/well and incubated at 37 ˚C with 5% CO_2 for 24 hr. For the control group, medium was replaced with complete medium containing $A\beta_{1-42}$ (5, 10, 20, 40, and 80 μmol·l^{-1}) and cultured for another 24 hr. For the HLJDD group, medium was replaced with complete medium containing HLJDD serum (0, 5, 10, 15, 20, 25, and 30%) and incubated for 24 hr. After incubation, 20 μl of 5 mg·ml^{-1} MTT was added to each well, followed by 4 hr of incubation at 37 ˚C. Absorbance at 490 nm was measured, and cell viability was calculated to determine the optimal $A\beta_{1-42}$ induction concentration and HLJDD intervention concentration.

Cell grouping

Cells were divided into the following groups. Blank group: HT22 cells were seeded into cell culture plates or glass-bottom culture dishes at a density of 104 cells per well, and cultured in a 37 ˚C incubator with 5% CO_2 for 24 hr. Model group: HT22 cells were cultured in complete medium containing 10 μmol·l^{-1} $A\beta_{1-42}$ for 24 hr to establish the AD cell model. Drug intervention group: HT22 cells were first cultured in complete medium containing 10 μmol·l^{-1} $A\beta_{1-42}$ for 24 hr. After that, the medium was aspirated, and the cells were then treated with complete medium supplemented with 15% HLJDD-containing serum for another 24 hr.

Determination of intracellular ROS levels

Cells in the logarithmic growth phase were seeded into glass-bottom culture dishes, and cultured and subjected to drug intervention according to the grouping method described in 1.4.3. After the culture of cells in each group was completed, the culture medium was aspirated, and the cells were washed once with HBSS buffer. Subsequently, an appropriate amount (sufficient to cover all cells) of 5 μmol·l^{-1} DCFH-DA was added, and the cells were stained at 37 ˚C in the dark for 30 min. After staining, the cells were washed twice with HBSS buffer, and then observed and photographed under a laser scanning confocal microscope.

Determination of intracellular mitochondrial membrane potential

Cells in the logarithmic growth phase were seeded into glass-bottom culture dishes, and cultured and subjected to drug intervention according to the grouping method. After the culture of cells in each group was completed, the culture medium was aspirated, and the cells were washed once with 500 μl of JC-1 buffer. Subsequently, the prepared JC-1 staining working solution was added, and the cells were incubated at 37 ˚C in the dark for 15 min. After incubation, the staining solution was aspirated, and the cells were washed once with JC-1 buffer. Hoechst 33342 staining solution was then added for nuclear counterstaining. Once counterstaining was finished, the staining solution was aspirated, and the cells were washed twice with JC-1 buffer. Finally, 500 μL of complete medium was added to the dishes, and the cells were observed and photographed under a laser scanning confocal microscope.

mRNA detection

The gene sequences of relevant factors on the National Center for Biotechnology Information (NCBI) were used as templates. The Primer 6.0 software was employed to design the amplification primer sequences for each factor. The primer sequences were as follows. For IP3R: Forward 5'-CGTTTTGAGTTTGAAGGCGTTT-3', Reverse 5'-CATCTTGCGCCAATTCCCG-3';For GRP75: Forward 5'-ATGGCTGGAATGGCC TTAGC -3', Reverse 5'-ACCCAAATCAATACCAACCACTG -3'; For VDAC1: Forward 5'- CCCACATACGCCGATCTTGG -3', Reverse 5'- GTGGTTTCCGTGTT GGCAGA -3'.Total RNA of cells in each group was extracted using Trizol reagent. The concentration of RNA was measured by a spectrophotometer. RNA was reverse-transcribed into cDNA through a two-step method. Then, the fluorescence quantitative PCR reaction was carried out with cDNA as the template.

Detection of protein expression levels

Cells in the logarithmic growth phase were seeded into cell culture plates, and cultured and subjected to drug intervention according to the grouping method. After the culture was completed, total cellular protein was extracted, and the protein concentration of each group was determined by the BCA method. An appropriate volume of 5× Loading Buffer was added to the protein samples of each group, and the mixtures were denatured at 95 ˚C for 10 min for subsequent use. A 10% SDS-PAGE gel was prepared, and 10 μg of protein was loaded into each lane. After electrophoresis, the protein blots were transferred onto PVDF membranes. The parameters for electrophoresis and membrane transfer were set as follows: 120 V for 80 min (electrophoresis) and 300 mA for 90 min (membrane transfer). The primary antibodies against VDAC1, GRP75, and IP3R were all diluted at a ratio of 1:1000, and the secondary antibody

was diluted at a ratio of 1:10000. β-actin was used as the internal reference. After developing with ECL developer, the membranes were detected by a chemiluminescence imaging system. The gray value analysis of the results was performed using ImageJ software.

ER-mitochondria fluorescence co-localization

Cells in the logarithmic growth phase were seeded into glass-bottom culture dishes, and cultured and subjected to drug intervention. After the culture was completed, the cells were taken out, and washed once with 1 ml of HBSS buffer. An appropriate amount of Mito-Tracker and ER-Tracker staining solutions was diluted with HBSS buffer at ratios of 1:5000 and 1:1000, respectively. The diluted staining solutions were then added to the culture dishes of cells in each group, followed by incubation at 37 ˚C in the dark for 30 min. The staining solutions were removed, and the cells were washed once with HBSS buffer. Hoechst 33342 staining solution was added for 15 min of staining. After that, the cells were washed twice with HBSS buffer and observed under a laser scanning confocal microscope. ImageJ plugin was used to perform Pearson's correlation coefficient analysis for co-localization on the images.

Detection of intracellular Ca^{2+} levels

Cells in the logarithmic growth phase were seeded into glass-bottom culture dishes, and cultured and subjected to drug intervention. Rhod-2, AM was diluted to 10 μmol·l^{-1} with HBSS buffer to prepare the staining working solution. The culture medium was aspirated, and the cells were washed once with HBSS buffer. Then, the Rhod-2, AM working solution was added to fully cover the cells, followed by incubation at 37 ˚C in the dark for 30 min. The staining solution was aspirated, and culture medium was added for another incubation at 37 ˚C in the dark for 30 min. After that, the cells were washed twice with HBSS buffer, and observed and photographed under a laser scanning confocal microscope.

Detection of cell apoptosis rate

Cells were cultured and subjected to drug intervention. After the culture was completed, cells in each group were resuspended and transferred to centrifuge tubes. Cells were collected by centrifugation at 300×g for 5 min, and each tube was added with 1 ml of PBS buffer for one wash. Cells were then resuspended and counted. A total of 106 cells from each group were added to flow cytometry sample tubes, followed by the addition of 100 μl Annexin V Binding Buffer to resuspend the cells. Subsequently, 2.5 μl of Annexin V-FITC Reagent and 2.5 μl of PI Reagent were added to the cell suspension. After gentle mixing, the cells were incubated at room temperature in the dark for 20 mi. After incubation, cells were centrifuged at 300×g for 5 min, and 500 μl of Annexin V Binding Buffer was added. After mixing, cell apoptosis was detected by flow cytometry, and the apoptosis rate of cells in each group was calculated based on the detection results.

Results

Effects of $A\beta_{1-42}$ and HLJDD on HT22 cell viability

To determine the optimal experimental concentrations of $A\beta_{1-42}$ and HLJDD for the present study, we first assessed the impact of HLJDD-containing serum on the viability of HT22 cells exposed to $A\beta_{1-42}$. As depicted in Figure 1A, HT22 cell viability declined significantly in a concentration-dependent manner with the escalation of $A\beta_{1-42}$ treatment. In contrast, the addition of 5% HLJDD-containing serum led to an increase in cell viability (Figure 1B). Based on these findings, 10 μmol·l^{-1} $A\beta_{1-42}$ was selected as the concentration for inducing cellular apoptosis, while 15% HLJDD-containing serum was designated as the drug intervention concentration for subsequent experiments in this study.

Effect of HLJDD on Intracellular ROS Levels

Intracellular ROS levels were quantified using the DCFH-DA assay kit. As presented in Figure 2, $A\beta_{1-42}$ induction led to a significant elevation in intracellular ROS levels compared to the control. In contrast, subsequent intervention with HLJDD-containing serum resulted in a gradual reduction in intracellular ROS accumulation. These observations confirm that HLJDD-containing serum exerts a ROS-scavenging effect, effectively lowering intracellular ROS levels in the $A\beta_{1-42}$-induced cell model.

Effect of HLJDD on mitochondrial membrane potential

Compared with the control group, the model group exhibited a significant decrease in the ratio of JC-1 polymers

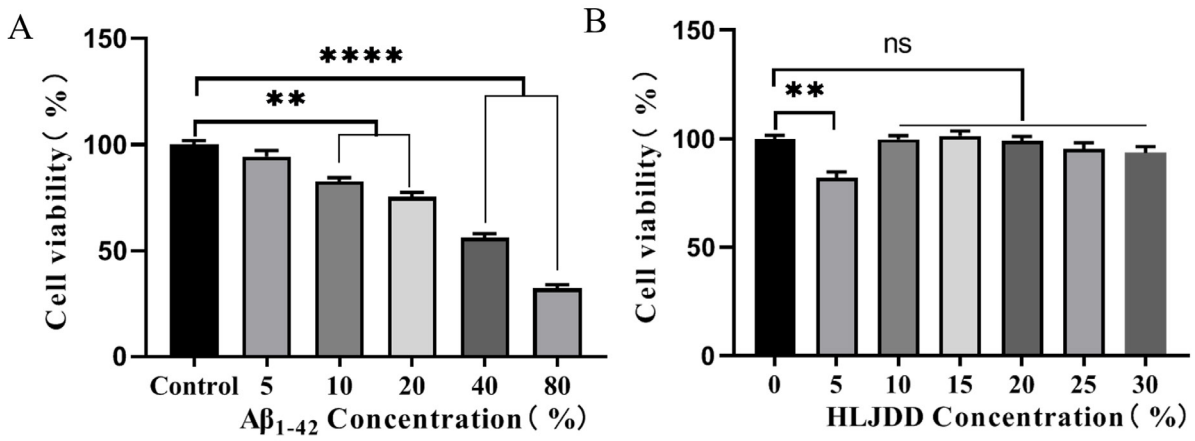

Figure 1. (A) Effect of Aβ1-42 on cell viability; (B) Effect of huanglian jiedu decoction (HLJDD) on cell viability
**P<0.01, ****P<0.0001, ns: no significance vs control group

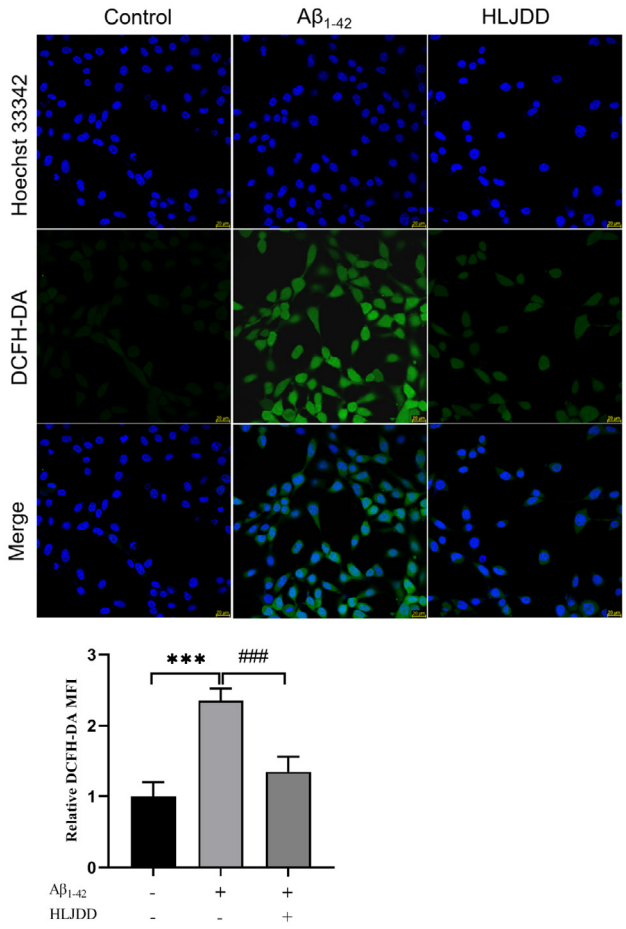

Figure 2. HT22 cells reactive oxygen species (ROS) levels were detected using DCFH-DA (400×)
In the AD cell model (10 μmol·L^{-1} $Aβ_{1-42}$), the ROS level was significantly increased (P<0.001); after intervention with HLJDD (15%), the ROS level decreased gradually (P<0.001). Scale bar=20 μm

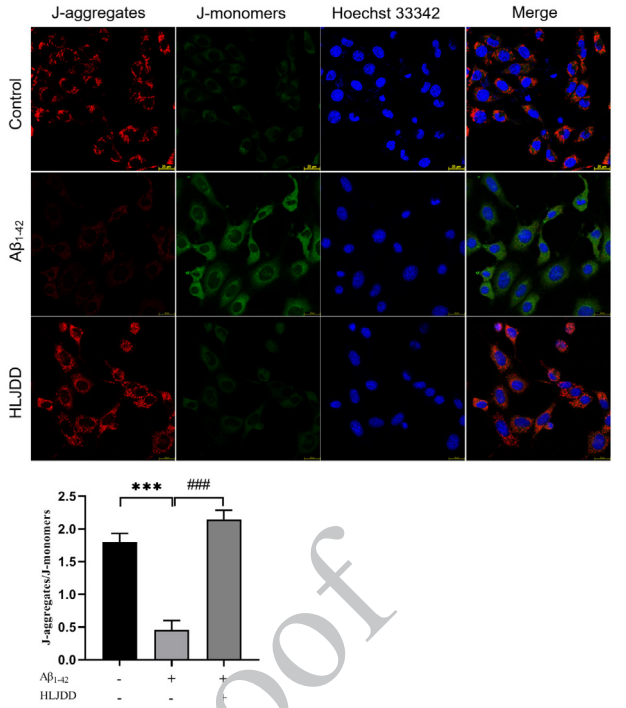

Figure 3. Effect of on mitochondrial membrane potential (MMP)
MMP was detected in HT22 cells using the JC-1 probe (630×). In the AD cell model treated with 10 μmol·L^{-1} $Aβ_{1-42}$, JC-1 J-aggregates decreased while J-monomers increased, indicating a decrease in MMP (P<0.001). Following intervention with HLJDD, J-aggregates increased by 15% and J-monomers decreased, corresponding to an increase in MMP (P<0.001). Scale bar=20μm

to monomers. Following intervention with HLJDD-containing serum, the ratio of JC-1 polymers to monomers was notably elevated. This result in Figure 3 demonstrates that HLJDD-containing serum is capable of restoring and increasing intracellular mitochondrial membrane potential in the $Aβ_{1-42}$-induced cell model.

Effect of HLJDD on mRNA Levels of various factors

Compared with the blank group, the model group showed significant up-regulation of VDAC1 and IP3R mRNA expression and down-regulation of GRP75 mRNA expression (Figure 4). After intervention with HLJDD-containing serum, VDAC1 and IP3R mRNA levels gradually decreased (P<0.01 or P<0.001), while GRP75 mRNA expression increased.

Effect of HLJDD on protein expression levels of various factors

As depicted in Figure 5, compared with the blank group, the model group displayed significant up-regulation of VDAC1 and IP3R protein expression and a significant down-regulation of GRP75. With HLJDD-containing serum intervention, VDAC1 and IP3R expression decreased, while GRP75 expression increased significantly.

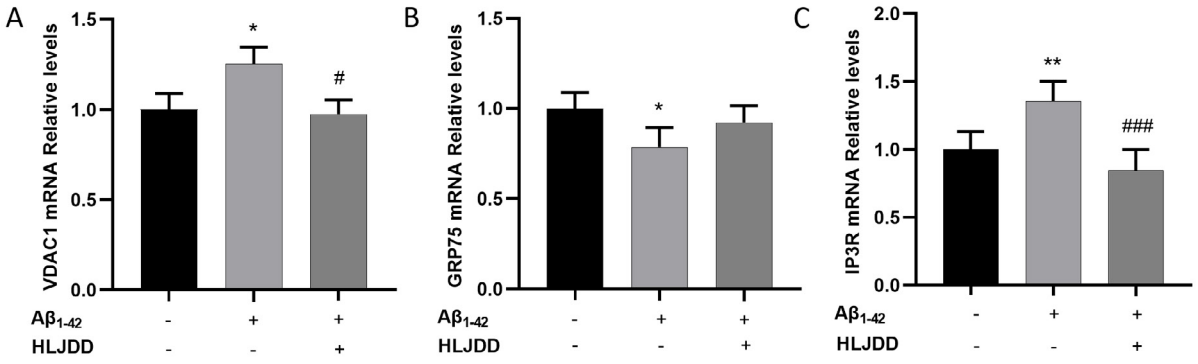

Figure 4. Effect of huanglian jiedu decoction (HLJDD) on mRNA of VDAC1 (A), GRP75 (B), and IP3R (C)
Data are expressed as mean±SD (n=3). *P<0.05, **P<0.01, ###P<0.001 vs control group

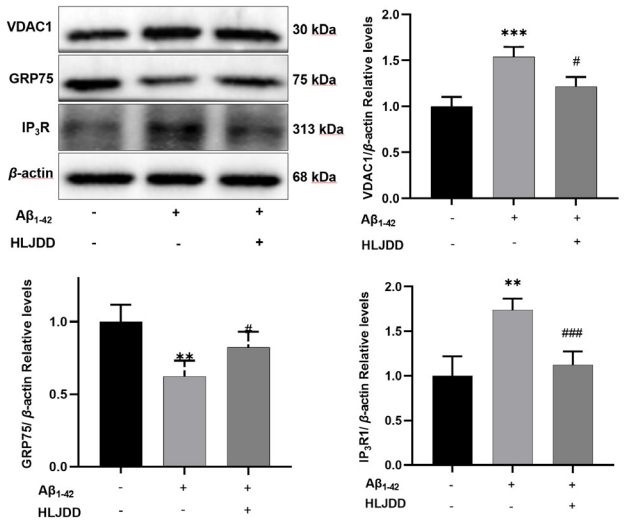

Figure 5. Effect of huanglian jiedu decoction (HLJDD) on protein expression of VDAC1, Grp75 and IP3R
#P<0.05, **P<0.01, ###P<0.001, ***P<0.001 vs control group

Effect of HLJDD-containing serum on MAMs structure

Laser scanning confocal microscopy was employed to visualize the co-localization of mitochondria (labeled with red fluorescence) and ER labeled with green fluorescence in $A\beta_{1-42}$-induced HT22 cells (Figure 6). Quantitative analysis revealed that the Pearson correlation coefficient and Mander's overlap coefficient for mitochondria-ER co-localization was significantly elevated in the $A\beta_{1-42}$-induced cells compared to the control. This increase in the Pearson coefficient and Mander's coefficient is a direct indicator of enhanced mitochondria-ER co-localization, which corresponds to an augmented formation of MAMs structures.

Effect of HLJDD on intracellular Ca^{2+} content

Laser scanning confocal microscopy was used to assess intracellular Ca^{2+} levels in $A\beta_{1-42}$-induced HT22 cells, with Ca^{2+} visualized via red fluorescence signals. Results in Figure 7 showed that the intensity of red Ca^{2+} fluorescence was significantly enhanced in $A\beta_{1-42}$-induced cells compared to the control. This marked increase in fluorescent intensity indicates that $A\beta_{1-42}$ induction disrupts intracellular Ca^{2+} homeostasis, triggering abnormal accumulation of Ca^{2+} and ultimately leading to intracellular Ca^{2+} overload— a key driver of cellular damage in the AD cell model.

Effect of HLJDD on cell apoptosis

As shown in Figure 8, compared with the control, the model group exhibited a significant increase in apoptotic cells (18.23%), which can be attributed to $A\beta_{1-42}$-induced excessive formation of MAMs structures and subsequent intracellular Ca^{2+} overload. Notably, after intervention with HLJDD-containing serum, intracellular Ca^{2+} levels in HT22 cells were reduced, accompanied by a marked decrease in the apoptosis rate to 7.32%. This finding further supports that HLJDD alleviates $A\beta_{1-42}$-induced cellular injury by mitigating Ca^{2+} overload, thereby suppressing apoptotic processes.

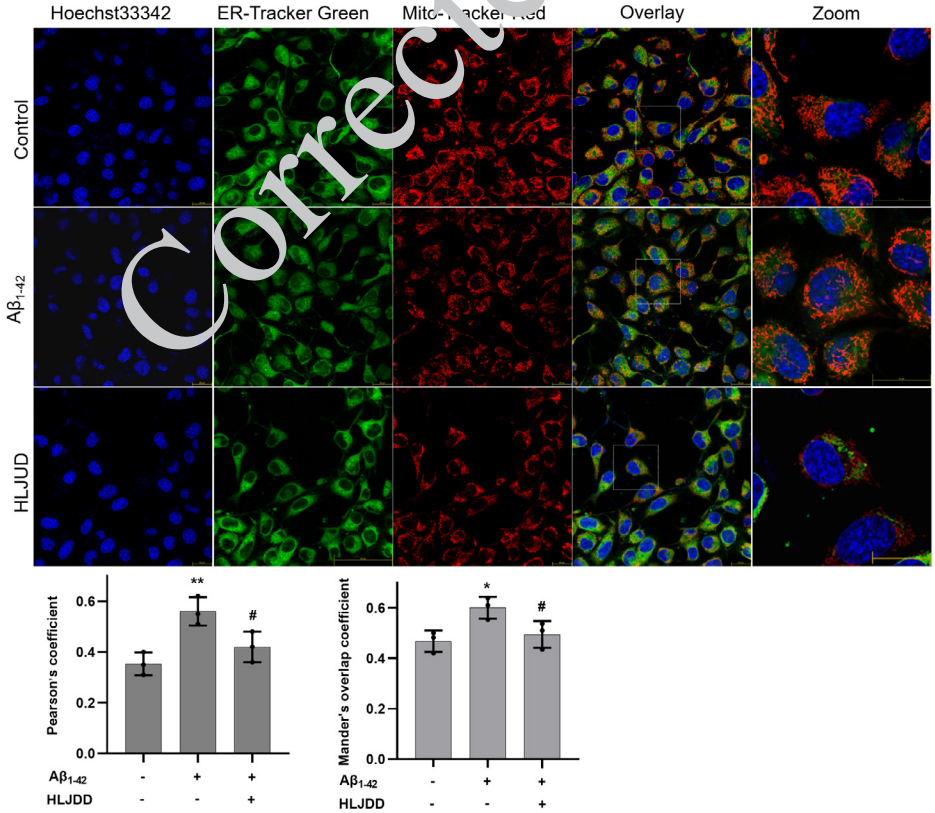

Figure 6. Effect of huanglian jiedu decoction (HLJDD) on the structure of mitochondria-associated endoplasmic reticulum membranes (MAMs)(630×)
Mitochondria-ER contact sites were assessed in cells using Mito-Tracker Red and ER-Tracker Green. In the Alzheimer's disease (AD) model treated with 10 μmol·l^{-1} $A\beta_{1-42}$, both the Pearson correlation coefficient (PCC) and Manders' overlap coefficient (MOC) for the co-localization of red (mitochondria) and green (ER) signals were increased, indicating more mitochondria-associated ER membranes (MAMs) and higher overlap between the organelles. After intervention with HLJDD (15%), PCC and MOC decreased, suggesting a reduction in MAM formation and diminished co-localization

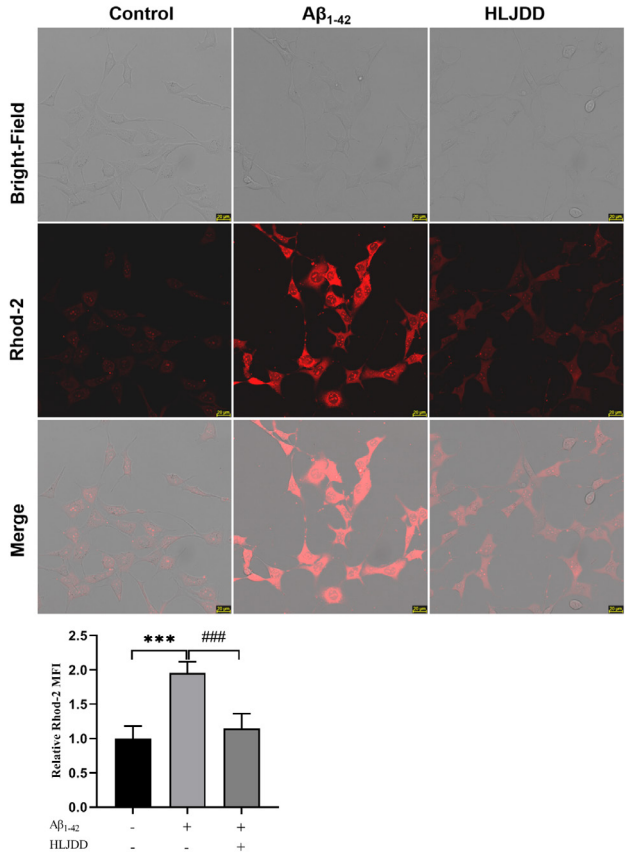

Figure 7. Effect of huanglian jiedu decoction (HLJDD) on intracellular Ca^{2+} (630×)
Intracellular Ca^{2+} content in HT22 cells was measured with Rhod-2/AM. In the AD cell model treated with 10 μmol·l^{-1} $A\beta_{1-42}$, red fluorescence indicating Ca^{2+} was significantly elevated (P<0.001), reflecting disrupted calcium homeostasis, intracellular Ca^{2+} overload, and consequent cellular damage. Following intervention with HLJDD (15%), intracellular Ca^{2+} levels decreased (P<0.001), indicating partial restoration of calcium homeostasis. Scale bar = 20 μm

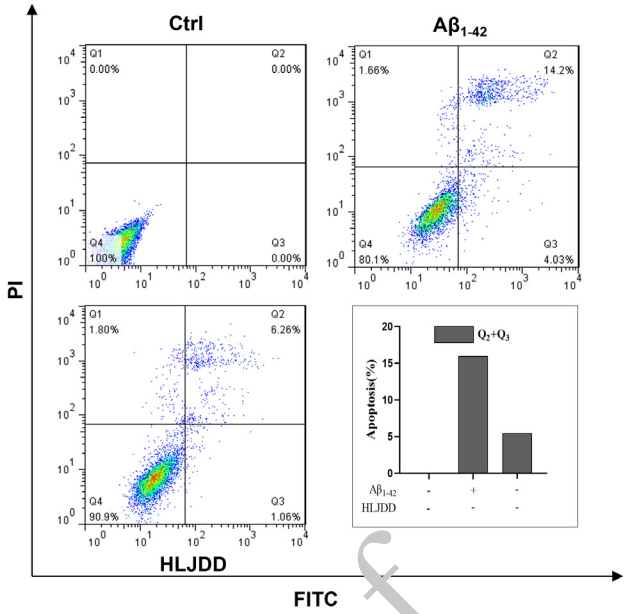

Figure 8. Effect of huanglian jiedu decoction (HLJDD) on cell apoptosis

Discussion

Ca^{2+} dynamics under physiological and pathological conditions is critical for unraveling the mechanisms of neurological diseases (19). AD pathogenesis remains incompletely understood, while Aβ accumulation and tau hyperphosphorylation were traditionally considered core drivers, dysregulated Ca^{2+} signaling and its downstream pathological cascades have emerged as central focuses in AD research (20).

MAMs act as key platforms for ER-mitochondria crosstalk, enriched with regulatory proteins (IP3R, VDAC1, Grp75) that govern Ca^{2+} transport, lipid metabolism, and mitochondrial dynamics (5-7). In this study, in the AD cell model induced by $A\beta_{1-42}$, the Pearson correlation coefficient for ER-mitochondria co-localization was increased; meanwhile, protein expression levels of IP3R and VDAC1 were elevated, whereas the expression of GRP75, a connecting protein between IP3R and VDAC1was down-regulated. This phenomenon may be related to the reduced distance between the ER and mitochondria, which facilitates Ca^{2+} transfer. After intervention with HLJDD, the ER-mitochondria co-localization coefficient decreased. Concurrently, the protein expression of IP3R and VDAC1 in MAMs was reduced, while the protein level of GRP75 was increased. These results indicate that intervention with HLJDD-containing serum can affect the formation of MAMs and alleviate damage in the cell model.

Consistent with these findings, $A\beta_{1-42}$ induction increased intracellular ROS, impaired mitochondrial membrane potential, triggered Ca^{2+} overload, and elevated apoptosis. HLJDD intervention mitigated ROS accumulation, restored mitochondrial function, reduced intracellular Ca^{2+} levels, and lowered the apoptosis. These results extend previous reports on HLJDD's neuroprotective effects by identifying a novel mechanism: HLJDD targets MAMs-mediated Ca^{2+} homeostasis to alleviate $A\beta_{1-42}$-induced neurotoxicity. Despite these insights, the study has limitations. First, conclusions rely solely on *in vitro* HT22 cell experiments, lacking verification from *in vivo* experiments. Second, experiments to block MAMs formation for verifying the drug's effect were not conducted. These limitations may restrict the comprehensive understanding of the mechanism by which HLJDD prevents and treats AD.

Conclusion

In summary, our study provides experimental evidence that HLJDD ameliorates $A\beta_{1-42}$-induced neurotoxicity by regulating MAMs function and restoring Ca^{2+} homeostasis, offering a novel mechanistic basis for its potential in AD therapy. Future *in vivo* studies and MAMs-targeted causality experiments will further validate these findings and advance the translational potential of HLJDD for neurodegenerative diseases.

Acknowledgment

This work was supported by Scientific and Technological Project of Henan Province (232102310505) and Special Project of Scientific Research on Traditional Chinese Medicine of Henan Province (2024Y1031).

Authors' Contributions

Y Y helped with writing the original draft, investigation, data curation, and conceptualization; Z L and J S provided methodology, and helped review, edit, and acquire funds; R W and H Z performed data curation and investigation.

Conflicts of Interest

The authors declare no competing financial interests.

Declaration

We have not used any AI tools or technologies to prepare this manuscript.

References

1.Alzheimer's Disease International. World Alzheimer Report 2023 (EB/OL). (2023-09-21). https://www.alzint.org/u/World-Alzheimer-Report-2023.
2. 2023 Alzheimer's disease facts and figures. Alzheimers Dement 2023; 19: 1598-1695.
3. Zhang Y, Chen H, Li R, Sterling K, Song W. Amyloid β-based therapy for Alzheimer's disease: Challenges, successes and future. Signal Transduct Target Ther 2023; 8: 248.
4. Congdon EE, Sigurdsson EM. Tau-targeting therapies for Alzheimer disease. Nat Rev Neurol 2018; 14: 399-415.
5. Wang N, Wang C, Zhao H, He Y, Lan B, Sun L, Gao Y. The MAMs structure and its role in cell death. Cells 2021; 10: 657.
6. Liu J, Yang J. Mitochondria-associated membranes: A hub for neurodegenerative diseases. Biomed Pharmacother 2022; 149: 112890.
7. Area-Gomez E, Schon EA. On the pathogenesis of Alzheimer's disease: The MAM hypothesis. FASEB J 2017; 31: 864-867.
8. Yu W, Jin H, Huang Y. Mitochondria-associated membranes (MAMs): A potential therapeutic target for treating Alzheimer's disease. Clin Sci (Lond) 2021; 135: 109-126.
9. Yao Xinmin, Li Xinxin, Zhou Jia, Wang Qi, Liu Guangzhou, Zhou Yanyan. Experimental research progress on Traditional Chinese Medicine in treatment of Alzheimer's Disease by regulating and controlling calcium ions in steady state. Chin Arch Tradit Chin Med 2018; 36: 49-52.
10. Annunziata I, Sano R, d'Azzo A. Mitochondria-associated ER membranes (MAMs) and lysosomal storage diseases. Cell Death Dis 2018; 9: 328.
11. Marchi S, Patergnani S, Missiroli S, Morciano G, Rimessi A, Wieckowski MR, *et al*. Mitochondrial and endoplasmic reticulum calcium homeostasis and cell death. Cell Calcium 2018; 69: 62-72.
12. Li Jinying, Huang Qihui, Tao Yangu. The effect of Naohuandan on learning and memory function and intracellular calcium ion concentration in the hippocampal region of APP/PS1 double transgenic mice. J New Chin Med 2014; 46: 213-216.
13.Liu Baoguang, Xie Miao, Dong Ying, Wu Hua, Li Yucheng, Pang Huijuan, *et al*. Research progress on mechanism of Huanglian Jiedu Decoction. Acta Chin Med 2022; 37: 1861-1868.
14.Wang Fan, Cen Xiaoguang. The advance of Huanglian jiedu Decoction in prevention and cure of senile dementia. J Liaoning Univ Tradit Chin Med 2015; 17: 4.
15. Xie Shuling, Peng Liyan, Yang Kun, Li Bin, Wu Wenbin. Research progress on the mechanism of Huanglian Jiedu Decoction in treating Alzheimer's Disease. Chin J Inf Tradit Chin Med 2014; 21: 121-123.
16. Zhang Yinghua, Lv Hanlin, Zhou Jianwen, Fan Li, Li Yang. Huanglian Jiedutang regulates HIF-1α/VEGF signaling pathway to improve learning and memory abilities of APP/PS1 transgenic mice. Chin J Exp Tradit Med Formulae 2024; 30: 59-65.
17. Wang Junli, Zhang Huifang, [illegible] Xinzi, Wang Rui, Du Yaming, Liu Xin, *et al*. Mechanism study of Huanglian Jiedu Decoction improving neuronal damage in Tau/ APP / PS1 Transgenic AD Mice by Inhibiting NLRP3 inflammasome. J Basic Chin Med 2024; 30: 986-991.
18. Zhang Libin, Meng Yingbing, Xu Xinzi, Wang Rui, Zhang Zhuo, Ma Zuofeng. The effect of Huanglian Jiedu Decoction on astrocytic ODC1 and its potential role in learning and memory in APP/PS1 mice. J Sichuan Tradit Chin Med 2024; .
19. Cárdenas C, Miller RA, Smith I, Bui T, Molgó J, Müller M, *et al*. Essential regulation of cell bioenergetics by constitutive InsP3 receptor Ca^{2+} transfer to mitochondria. Cell 2010; 142: 270-283.
20. Qi S, Yuan Y, Yang W, Su JY, Hao LY. Calcium dyshomeostasis and Alzheimer's Disease. Acta Acad Med Sin 2024; 46: 592-602.